SCIENTIFIC REPORTS

OPEN

SUBJECT AREAS:
CYTOGENETICS
HERPES VIRUS

Received
13 November 2013

Accepted
17 March 2014

Published
2 April 2014

Correspondence and requests for materials should be addressed to H.K. (kura@fujita-hu.ac.jp)

Dual roles for the telomeric repeats in chromosomally integrated human herpesvirus-6

Tamae Ohye[1], Hidehito Inagaki[1], Masaru Ihira[2,3], Yuki Higashimoto[2,4], Koji Kato[5], Junko Oikawa[6], Hiroshi Yagasaki[7], Takahiro Niizuma[8,9], Yoshiyuki Takahashi[10], Seiji Kojima[10], Tetsushi Yoshikawa[2] & Hiroki Kurahashi[1]

[1]Division of Molecular Genetics, Institute for Comprehensive Medical Science, Fujita Health University, Toyoake, Aichi 470-1192, Japan, [2]Department of Pediatrics, Fujita Health University School of Medicine, Toyoake, Aichi 470-1192, Japan, [3]Faculty of Clinical Engineering, Fujita Health University School of Health Sciences, Toyoake, Aichi 470-1192, Japan, [4]Department of Laboratory Medicine, Fujita Health University Hospital, Toyoake, Aichi 470-1192, Japan, [5]Department of Hematology and Oncology, Children's Medical Center, Japanese Red Cross Nagoya First Hospital, Nagoya, Aichi 453-8511, Japan, [6]Department of Pediatrics, Chiba University School of Medicine, Chiba, Chiba 260-8670, Japan, [7]Department of Pediatrics, School of Medicine, Nihon University, Itabashi-ku, Tokyo 173-8610, Japan, [8]Department of Pediatrics, Koshigaya Municipal Hospital, Koshigaya, Saitama 343-8577, Japan, [9]Department of Pediatrics, Tokyo Rinkai Hospital, Edogawa-ku, Tokyo 134-0086, Japan, [10]Department of Pediatrics, Nagoya University Graduate School of Medicine, Nagoya, Aichi 466-8550, Japan.

Approximately 1 percent of healthy individuals carry human herpesvirus-6 within a host chromosome. This is referred to as chromosomally integrated herpesvirus-6 (CIHHV-6). In this study, we investigated the chromosomal integration site in six individuals harboring CIHHV-6B. Using FISH, we found that HHV-6B signals are consistently located at the telomeric region. The proximal endpoints of the integrated virus were mapped at one of two telomere-repeat-like sequences (TRSs) within the DR-R in all cases. In two cases, we isolated junction fragments between the viral TRS and human telomere repeats. The distal endpoints were mapped at the distal TRS in all cases. The size of the distal TRS was found to be ~5 kb which is sufficient to fulfill cellular telomeric functions. We conclude that the viral TRS in the DR regions fulfill dual functions for CIHHV-6: homology-mediated integration into the telomeric region of the chromosome and neo-telomere formation that is then stably transmitted.

Human herpesvirus 6 (HHV-6) is one of the best characterized family members of the nine human herpesviruses. HHV-6 is classified as two distinct species, designated HHV-6A and HHV-6B, with an overall nucleotide sequence identity of 90%[1–3]. It has been demonstrated that primary HHV-6B infection occurs in infancy and causes a common febrile exanthematous illness, exanthem subitum[4,5]. However, neither the clinical features of primary HHV-6A infection nor the diseases directly associated with it have been identified to date. Following primary infection, HHV-6 remains latent in monocytes/macrophages and persists in the salivary glands[6,7]. In transplant recipients, HHV-6B reactivation can cause several clinical conditions such as encephalitis, bone marrow suppression, and pneumonitis[8,9].

Accumulating evidence now indicates that a subset of normal healthy individuals carry the HHV-6 genome within their chromosomes, which is known as chromosomally integrated herpesvirus-6 (CIHHV-6)[10]. The virus genome in these cases is transmitted by Mendelian inheritance. The integrated virus itself does not appear to be pathogenic, but CIHHV-6 carriers are often identified as high-titer virus carriers during screenings for HHV-6 reactivation in immunocompromised hosts. The presence of CIHHV-6 is not a rare condition with a reported incidence in healthy individuals of 1% in Caucasians and 0.21% in Japanese populations[11–13].

Based on consistently detectable FISH signals at chromosome ends in all previously analyzed independent CIHHV-6 cases, it had been speculated that the HHV-6 viral genome is integrated into human telomeres through an unknown mechanism that is specific to HHV-6[14]. The HHV-6 genome comprises a linear double stranded DNA of 159 kb flanked by identical 8 kb direct repeats at the left and right ends (DR-L and DR-R). Each DR contains two human telomere repeat (TTAGGG)-like sequences (TRS) proximal to both ends of the DRs[15,16]. The function of these motifs is uncertain, but it is not unreasonable to hypothesize that they plays a role in protection of viral genome ends from host defense systems such as nucleases in a similar manner to the telomere protection

from DNA end repair systems in eukaryotes[17]. Recently, sequence analysis of the junction fragments of three individuals with CIHHV-6A revealed that the HHV-6 genome was directly joined with the human telomeric region via TTAGGG repeats in each case[18]. A homology-directed mechanism operated by host DNA damage repair response pathways such as homologous recombination is likely to mediate these rearrangements[19].

To further elucidate the mechanism of the viral integration into the human telomeres, we investigated the integration sites in six Japanese individuals harboring CIHHV-6B.

Results

Six cases that were suspected to CIHHV-6B by having genome-equivalent copy number of viral DNA in peripheral blood samples estimated by qPCR were analyzed[20]. Standard cytogenetic evaluations revealed no abnormalities in any of these subjects. FISH analysis with a HHV-6 genomic DNA probe detected virus-specific signals on the long arm of chromosome 22 in two cases (cases 18 and 19), on the long arm of chromosome 6 in one case (case 31), and on the short arm of chromosome X in the two cases (cases 28 and 63) (Fig. 1b–d). The mother of case 19 (case 20) was also analyzed and showed HHV-6 signals on the long arm of chromosome 22. Thus, a CIHHV-6B diagnosis was confirmed in all six study subjects. CIHHV-6B FISH signals were detectable on only one of the homologues in each case, suggesting that all six individuals were heterozygotes in terms of viral integration. HHV-6 signals were consistently detected at the end of the chromosomes, presumably at the telomeric regions, in all six cases.

To next determine the structure of the integrated viral genome in our subjects, we performed MLPA experiments which allowed us to determine copy number of the target sites of the viral genome relative to the chromosomal DNA in each case. The copy numbers for the UL regions were constant and similar to the chromosomal regions used as references (Fig. 2), suggesting that a single copy of the viral genome was integrated within the chromosomal DNA in our CIHHV-6 cases. Copy numbers for the DRs varied among the subjects; two-fold higher than those for the UL regions in cases 18, 19, and 20, three-fold higher in case 28, and at a similar level in case 31.

To map the breakpoints of the HHV-6 integration in more detail in our subjects, Southern analyses using several HHV-6 probes were performed. Since the two TRS regions in the DR-R are good candidates for viral integration breakpoints, DR probes located near to the TRS-2 site were used (Supplementary Fig. S1). These DR probes yielded two distinct bands of a similar intensity (Fig. 3a). One of the bands was detected at a similar position in all cases with a size that was expected for the DR-L, suggesting that the DR-L was intact. The sizes of second band were different in each case, although two cases that were found to carry the HHV-6B at the long arm of chromosome 22 showed a second band of similar size. This suggests that these fragments included the junction between the viral and human genome. According to the restriction map, the breakpoints were predicted to be located within the TRS-2. A similar band pattern in two cases with a 22q integration indicated a common founder for this integration event. The fact that two bands were detectable in these analyses suggests that the entire viral genome was inserted together with both the DR-L and DR-R. The fact that the intensities of the two detected bands were similar further supports the idea that only a single copy of entire HHV-6B genome had been inserted in each individual.

We next attempted to isolate the junction fragments and could fortunately rely on sequence information for the subtelomere-telomere junction in the Xp region. First, we performed PCR using a primer designed to amplify the subtelomeric region flanking the telomere repeats and a primer that recognized the UL region just outside of the DR-R. The amplification reactions appeared to yield no product, but subsequent Southern hybridization analysis detected

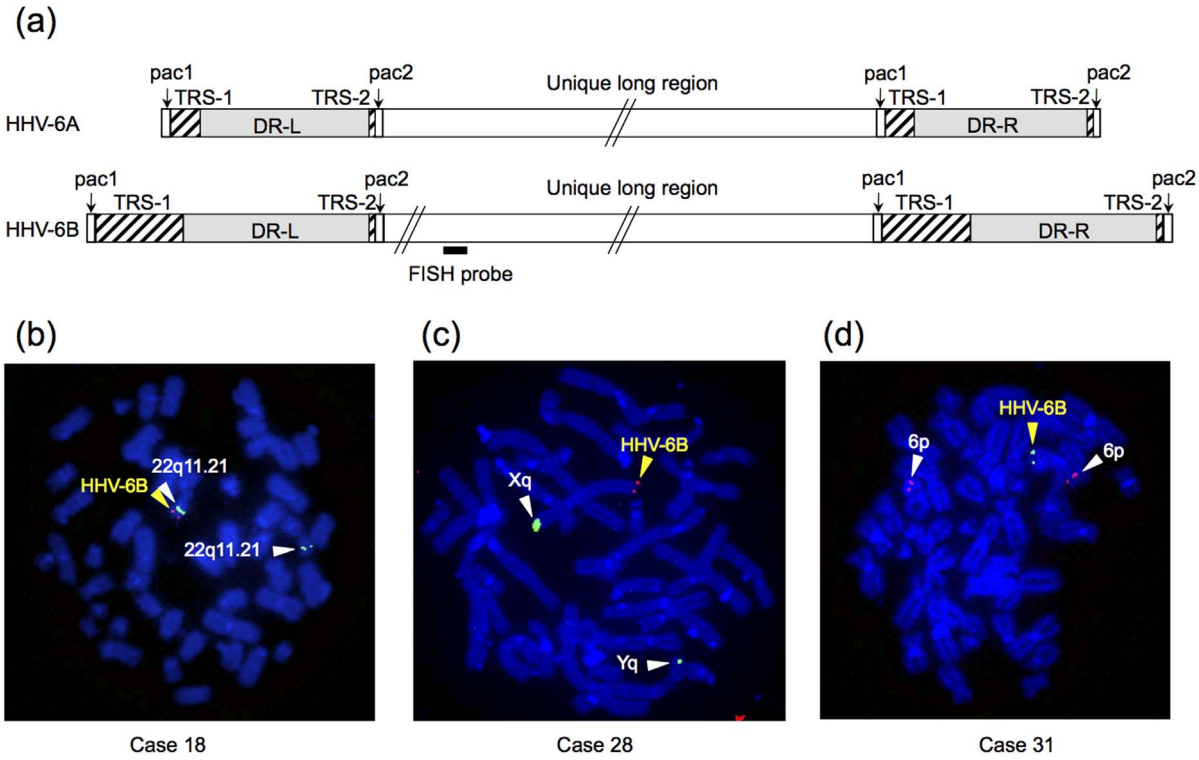

Figure 1 | Characterization of CIHHV-6B by FISH. (a) Schematic representation of the HHV-6 genomic structure. The 10 kb Pst I fragment used as s FISH probe is indicated. Gray boxes indicate DR sites and hatched boxes indicate TRS regions. (b) FISH analyses of metaphase chromosomes derived from the CIHHV-6B study subjects. A signal from the HHV-6B probe is detectable at the end of chromosome 22q (case 18), chromosome 6q (case 31) or chromosome Xp (case 28) (yellow arrowheads). The reference signals for chromosome 22q11.21, 6p and Xq are indicated by white arrowheads.

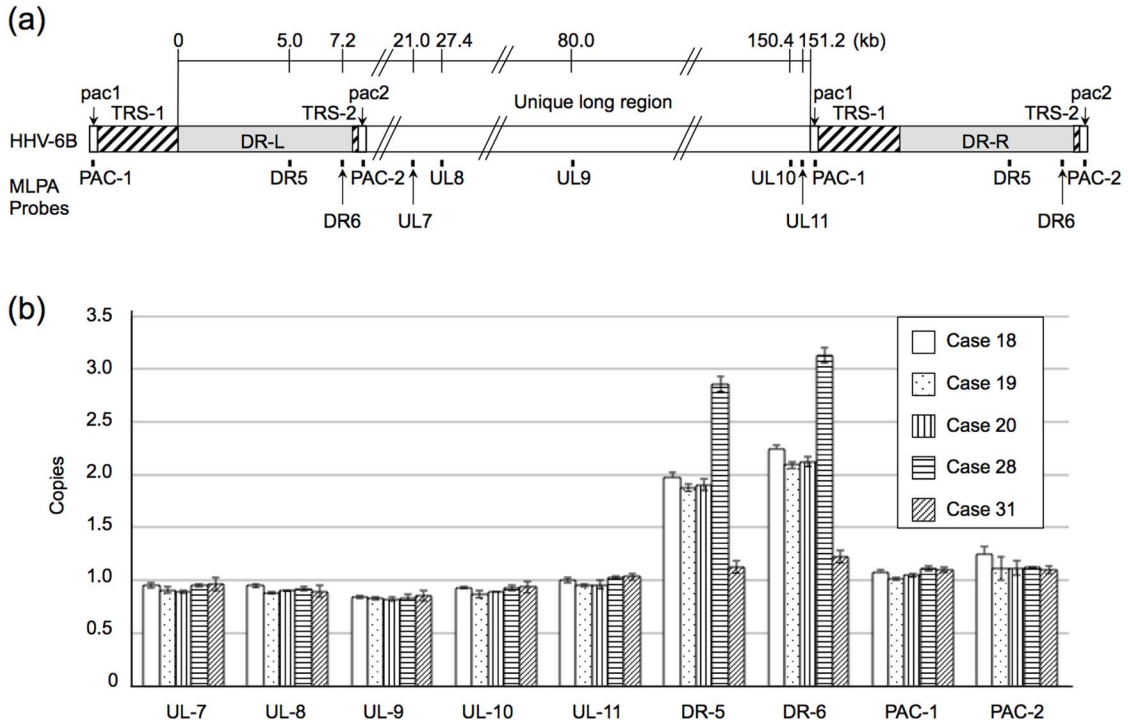

Figure 2 | Analyses of the CIHHV-6B genome structure by MLPA. (a) Schematic representation of the HHV-6B genome. The positions of the MLPA probes are indicated below the diagram. The scale bar indicates the distance from the starting point of DR-L. (b) Results of MLPA analyses. The vertical axis indicates the viral genome copy numbers relative to the single copy human genomic region. Data for cases 18, 19, 20, 28 and 31 are indicated from left to right.

a fragment exceeding 10 kb in length in case 28 with a HHV-6 integration at chromosome Xp (Fig. 3b). This indicated that the breakpoints of the virus were located within the DR-R. Unfortunately, less sequence information was available for the subtelomeric regions of chromosomes 6q and 22q. We attempted to perform junction PCR using a primer that bound to the most distal end of the reported subtelomeric sequence and a primer that recognized a region just outside of the DR-R, but no amplicon was obtained. We also tried inverse PCR but failed, because a short PCR product derived from short TTAGGG repeat present in the DR-L inhibited the amplification of real junction.

To further narrow down the positions of the HHV-6 breakpoints, multiple PCR primers were designed within the DR. Combined with a subtelomeric primer designed on the basis of sequence information for the Xp subtelomere-telomere junction (hg19, chrX: 60,427–60,445), all of the primers that recognized sites within the DR yielded PCR products of the expected size, which confirmed that the viral breakpoint is located within the TRS-2 (Fig. 3c). Sequencing of these amplicons revealed that the subtelomeric and viral DR-R regions were connected via 166 copies of the TTAGGG repeat, which is much shorter than the typical telomere repeat region in humans (9-15 kb; Fig. 3d) (GenBank accession number AB822541). These PCR experiments also yielded junction products in case 63 who had a HHV-6 integration at chromosome Xp. The sequence of this amplified fragment indicated that the integration sites are identical and the differences in the PCR product sizes was due to varying numbers of telomere repeats.

In one of our study subjects (case 31), the results of MLPA revealed only one copy of the DR, which was a similar level to the UL. Southern hybridization results for case 31 also produced a distinct pattern. A DR probe detected no bands corresponding to the DR-R, but constant bands only corresponding to the DR-L, suggesting that the TRS-2 had been deleted and that the HHV-6 breakpoint is located at a more distal region in this subject (Fig. 3a). Since TRS-1 is another candidate for the viral breakpoint, PCR for this region was performed using a DR primer flanking the TRS-1 site and a primer that was located just outside of the DR-R. No PCR product was obtained for case 31 although a TRS-1 amplicon was obtained in all other subjects, suggesting that the breakpoint in this one subject was located within the TRS-1 site in the DR-R (Supplementary Fig. S2a). Unexpectedly, the sizes of the TRS-1 PCR products from other cases were much larger (~5 kb) than that reported in the database (~300 bp), and also than TRS-2 (~500 bp). Although TRS-1 is referred to as heterogeneous $(TTAGGG)_n$ due to the reported presence of imperfect repeats, sequence analyses of our study subjects revealed a much longer stretch of perfect TTAGGG repeats than has been previously reported for the TRS-1 site, and greater also than those of TRS-2.

In case 28, MLPA results revealed a three-fold higher copy number for the DR compared with the UL region. Southern analyses further demonstrated the presence of additional DR copies in this subject, evidenced by three distinct bands (Fig. 3a). Sizes of the restriction fragments detected by DR probes suggested a proximal-DR-DR-UL-DR-distal structure within the genome of this individual (Supplementary Fig. S1, S3, and S4). To reveal the junction of the two distal DRs in this case, we performed PCR encompassing the TRS-2 – pac2 – pac1 – TRS-1 region. Only case 28 yielded a junction-specific PCR product that was also yielded from the subject including the replicating HHV-6B obtained from patients with exanthema subitum (Supplementary Fig. S5a). However, sequence analyses revealed that the junction between the two DRs in case 28 did not include pac1 or pac2, although the junction from the replicating HHV-6B carried the pac1 and pac2 regions.

To determine the structure of the other end of the HHV-6B genome, we mapped the endpoint of the viral genome within the DR-L. PCR amplification of the TRS-2 site in the DR-L was performed, and amplicons were obtained for all of our CIHHV-6B subjects. This suggested that the TRS-2 region in the DR-L had remained intact

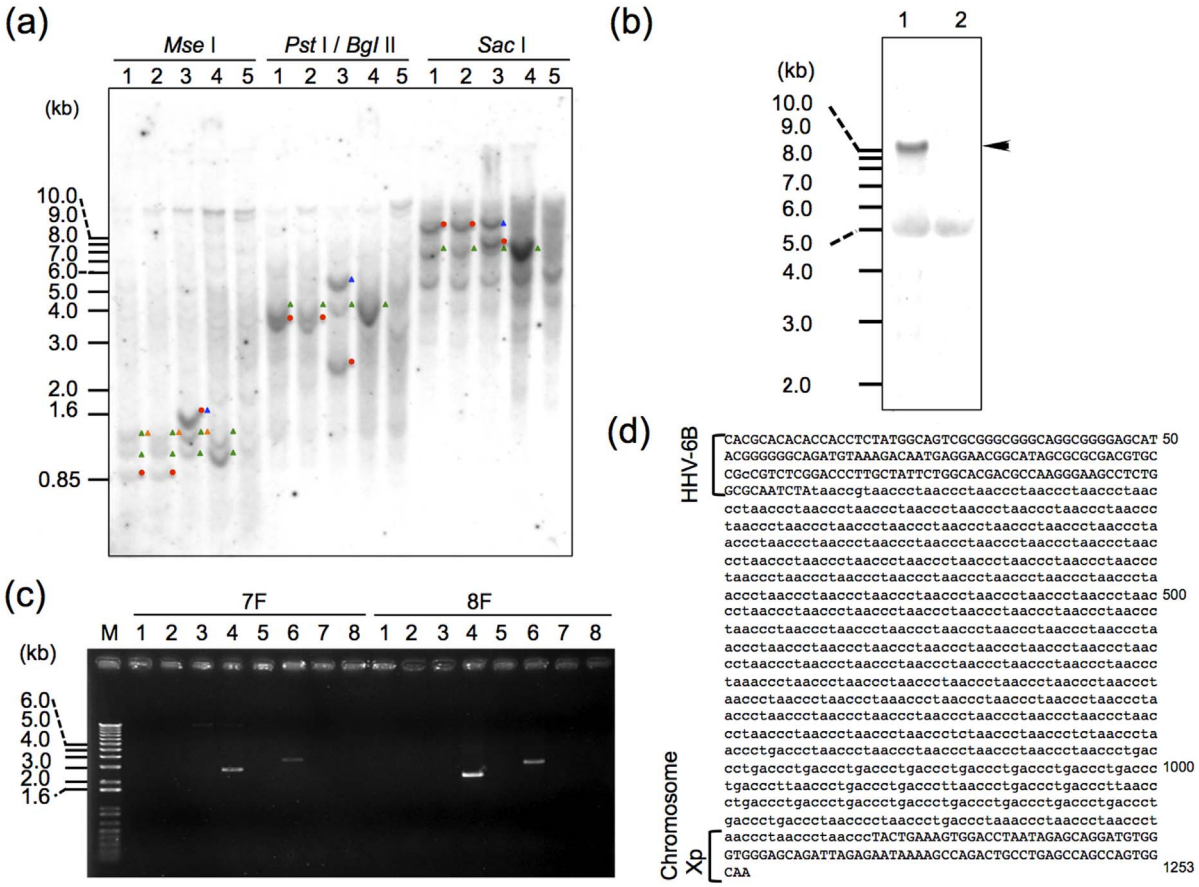

Figure 3 | Analyses of the junction between the human chromosome and viral genome. (a) Southern blot analyses of genomic DNA from the CIHHV-6B study subjects. The restriction enzymes used for these analyses are indicated above the panels; size markers are indicated on the left. Red dots indicate the rearranged bands derived from junction between human telomere and the HHV-6. Triangles indicate bands derived from the DR-L (green) and DR-R (orange), while blue triangles indicate the junction of the two DRs. Lane 1, case 18; lane 2, case 19; lane 3, case 28; lane 4, case 31; lane 5, non-CIHHV-6 control. (b) Southern blot analyses of PCR products. The arrowhead indicates a junction-specific PCR product. Lane 1, case 28; lane 2, non-CIHHV-6. Complete raw autoradiogram image can be seen in Supplementary Fig. S6. (c) PCR products that incorporate junction fragments. The primer sets were designed on the DR region (7F or 8F) and subtelomeric region on chromosomes X. Two CIHHV-6 cases yielded amplicons of different sizes. Lane M, size markers; lane 1, case 18; lane 2, case 19; lane 3, case 20; lane 4, case 28; lane 5, case 31; lane 6, case 63; lane 7, non-CIHHV-6 case; lane 8, water control. (d) Sequence of the junctions in case 28. The sequence shown covers the region from the DR-R of the viral genome to the human subtelomeric region. Lowercase letters denote telomere repeats.

in all cases (Supplementary Fig. S2b). We next performed PCR using one fixed primer for the site just outside of the DR-L and other primers for different sites within the DR. All of the primers within the DR successfully amplified specific products (Fig. 4). A telomere-repeat primer also yielded products appearing as a smear, the specificity of which was confirmed by Southern hybridization (Supplementary Fig. S5b). However, the use of a primer for the pac1 site did not yield any specific product. We also designed MLPA probes within the pac1 or pac2 region which produced a single copy signal which was similar to the UL region (Fig. 2), suggesting the absence of the pac1 site. These results demonstrated that the CIHHV-6B chromosome ends within the TRS-1.

The presence of the TRS-2 in the DR-L not only indicated an intact TRS-2, but also gave us the opportunity to analyze individual variations in the TTAGGG repeat numbers. As expected, the sizes of the PCR products varied among individuals (Supplementary Fig. S2b)[21]. Among three of our study subjects with an integration at 22q, two cases from the same family (cases 19 and 20) showed an amplified product of the same size. The other case with a viral integration at 22q (case 18) showed a PCR product of a similar size but subsequent sequence analysis revealed different numbers of telomere repeats (32 for cases 19 and 20 versus 29 for case 18). Two cases with a viral integration at Xp showed different numbers of repeats (27 for case 28 and 23 for case 63).

Discussion

In our present study, we analyzed the structure of the integrated HHV-6B genome in six carriers of this virus using the MLPA technique. Achieving accuracy in copy number measurements poses particular challenges when attempting to characterize a tandem repeat region. The MLPA method shows utility in reproducibly distinguishing two copies of repeats from a single copy, which is not easily achievable using other standard methods. MPLA also overcomes the instability of the qPCR technique due to its high sensitivity to the amounts of template DNA, and thereby yields reproducible results[22]. Hence, MLPA is often used for the identification of deletion/duplication mutations in disease-causing genes or for determining the status of copy number variations at certain chromosomal loci in humans. In our current study, the use of MLPA allowed us to clearly determine the copy number of the integrated HHV-6B genome in the carriers and to characterize structural variations in the integrated viral genome among these CIHHV-6B cases. Our data indicate that human telomere repeats and the viral genomes had fused via one of the two TRSs within the DR-R in all six cases and

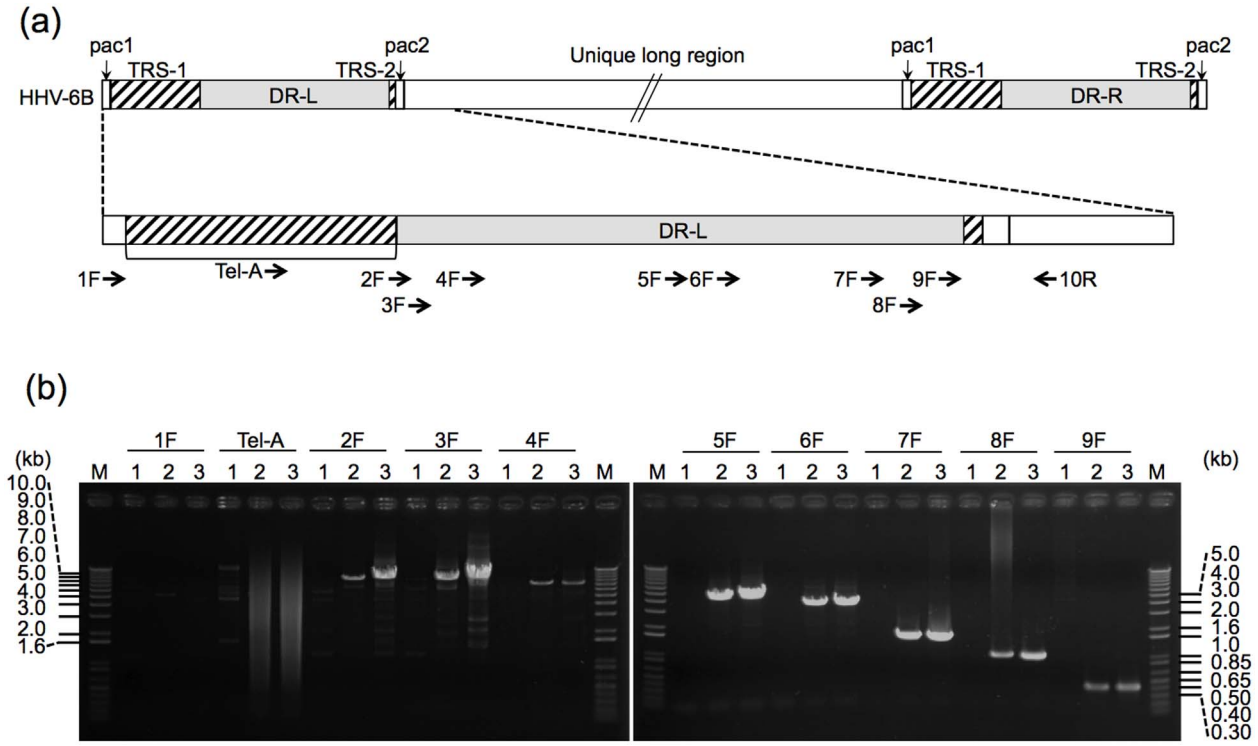

Figure 4 | Long range PCR analyses to determine the endpoints of the viral genomes. (a) Schematic representation of the HHV-6B genomic structure. The positions of the PCR primers are indicated below the diagram. (b) Results of long range PCR analyses. The 10R primer was used together with one of the DR primers for the long range PCR. The DR primers are indicated above the panels. Lane M, size markers; lane 1, non-CIHHV-6 case; lane 2, case 28; lane 3, case 18.

that the other end of the integrated HHV-6 virus is likely to be the distal TRS within the DR-L. Our findings are almost similar to those published previously[18,25]. These data implicate dual roles for the viral TRS sites in the manifestation of CIHHV-6.

The first important role of the viral TRS in the onset of CIHHV-6 is to trigger the homology-directed DNA repair mechanism for subsequent integration of the viral genome into the human genome. The ends of chromosomal DNA comprising the telomeres are generally structurally organized not to activate a DNA damage response by forming a stable T-loop DNA secondary structure and through the assembly of a shelterin complex[17]. Indeed, in normal cells, homologous recombination is repressed at the telomere[23]. However, the shortening of telomeres as a result of cell division might lead to a loss of chromosomal end protection and may cause improper DNA repair such as end-to-end fusions of the chromosomes by non-homologous end joining[24]. In our current study, the telomere repeats at the junction between the human subtelomere and the HHV-6 genome were found to be low in number, which has also been reported previously[18]. We thus speculate that telomere shortening, when it occurs in the cells infected with HHV-6, may activate a homology-directed DNA damage response that leads to viral integration.

A previous report has indicated that the viral breakpoints are located at TRS-2, both for CIHHV-6A and 6B[18,25]. The TRS-2 site has been shown to be longer and contain fewer degenerate TTAGGG repeats than TRS-1. However, our current analyses has revealed that the sizes of the TRS-1 region in our study subjects were much larger than TRS-2 and contained more perfect telomere repeats. If the free DNA end at the human telomere had activated the homology-directed DNA repair response pathway and searched for the appropriate template for DNA repair via homology, the integration event would have preferentially utilized TRS-1. However, we found that this was not the case. Thus, we speculate that the viral DNA end may be recognized as a bona fide DNA end by the host DNA repair system and thus subjected to end resection via homology-directed machinery. A small resection would be sufficient to reach the TRS-2 in the DR-R and enable the DNA end to find its homologous template, i.e. the human telomere. If the protection of the human telomere is incidentally removed at the time of this homology search due to age-related telomere shortening, the two DNA ends might be connected in a homology-dependent manner.

Once HHV-6 infection is established, the circularization of the linear double stranded viral DNA give rises to the formation of a stable episomal form in the nucleus whereby latency is achieved[26]. During HHV-6 replication, the episome produces a head-to-tail concatemer via a rolling circle mechanism, which is cleaved into a single unit of linear viral genome and is subsequently recircularized. A previous study has reported that some CIHHV individuals carry more than two copies of HHV[27]. However, in our current study we found only one copy of the viral genome in all of the CIHHV-6 cases in our cohort. In case 28, we identified tandem DRs repeat with no intervening pac1-pac2 region, which should be identified in a replicating concatemer or episomal virus. This suggests that a single linear form of replicated HHV-6 in latently infected cells gives rise to the integration event[10]. Normally, linear viral DNA ends are protected by episome formation, but it is possible that replication errors at the junction might result in an uncircularized virus genome, which may induce a DNA damage response. Although homologous recombination is suppressed at the telomere, a recent report has provided evidence of single strand annealing as a mechanism of telomere fusion[28].

The second pivotal role of the TRS regions in CIHHV-6 is the stabilization of the chromosomal end required for transmission of the virus. In our current analyses, we demonstrate that the end of the HHV-6B integrated chromosome was TRS-1, which others have also demonstrated using single telomere length analyses[25]. Once HHV-6 is integrated into the human telomere via homology with the TRS in the DR-R, the other end of the viral genome, DR-L, becomes a chromosomal end. Without the protection that normally operates

Table 1 | Characteristics of the Japanese study subjects with CIHHV-6B

Family	Case	Trigger for the diagnosis of CIHHV-6B	Chromosome
1	18	Monitoring after bone-marrow transplantation Aplastic anemia	22q
2	19	Differential diagnosis of mycoplasma Encephalitis	22q
	20	Mother of case19	22q
3	28	Monitoring after bone-marrow transplantation Congenital pure red cell aplasia	Xp
4	31	Differential diagnosis of febrile skin rash	6q
5	63	Uveitis	Xp

for chromosomal ends at the telomeres, the DR-L is subject to DNA end resection until the TRS-1 appears. Since the TRS-1 length is sufficient to recruit components of the shelterin complex, it can form a neo-telomere to maintain its size during some rounds of DNA replication and cell division until it forms gametes to transmit the viral genome to the offspring. We note that there is no reported case of chromosomally integrated HHV-7[29] and this might be due to a short TRS-1 (90 bp) in the genome of this virus which cannot maintain chromosomal end stabilization (U43400).

One of our current CIHHV-6B cases (case 31) was found to carry a different junction between the virus and human telomere, with a breakpoint in the TRS-1 region. One possibility for this occurrence is that a long DNA end resection took place that extended to the TRS1, which may be rare. Another possibility is a post-insertional genomic rearrangement[30]. Alternatively, non-allelic homologous recombination (NAHR) between the two TRS sites might have produced the deletion of DR-R in case 31, thereby mimicking the breakpoint at a different location for the initial integration. Another CIHHV-6B subject in our present analyses (case 28) was found to carry three DR copies. This is also possibly a product of an NAHR event between the two different TRS sites on the HHV-6 virus. In contrast to the normal repression of homologous recombination at the telomere, the subtelomeric region is known to be highly unstable and undergo frequent recombination[31]. The integration of HHV-6B in cases 28 and 63 in our present study are likely to have originated from a single ancestor since an identical genomic structure, three DR sites without a pac1-pac2 junction, was found in these two individuals. However, the repeat number at the TRS2-human telomere junction, as well as in the TRS2 site at the DR-L was found to be diverse between these two cases, suggesting that replication slippage or recombination may occur frequently at this new subtelomeric region.

A remaining question from our current observations is the timing of HHV-6 integration during the life cycle of a human host. Since CIHHV-6 appears to be transmitted from parent to child in a Mendelian fashion, the integration event must occur during germ cell development. HHV-6 uses CD46 as its receptor for entry into the cell[32]. Since CD46, a regulator of the complement activation receptor, is expressed ubiquitously, HHV-6 can theoretically infect all human cell types including those of a germ cell lineage. Since spermatogenic cells undergo a considerably greater number of DNA replication and cell division events than any other cells, there may be a higher chance of an integration event due to telomere dysfunction, although germ cells do possess telomerase activity[33]. Our current findings that some identified CIHHV-6 cases have similar molecular characteristics suggest that integration is a rare event. We propose from this that a small number of ancestral chromosomes that had undergone a HHV-6 integration have likely expanded throughout the general human population as a neutral polymorphism.

Methods

Human subjects. We analyzed six Japanese cases that were suspected to CIHHV-6B by having genome-equivalent copy number of viral DNA in peripheral blood samples estimated by qPCR[20]. The clinical features of the cases are listed in Table 1. After informed consent was obtained, peripheral blood samples were obtained again from each patient for our genomic analyses. Our study was approved by the Ethical Review Board for Human Genome Studies at Fujita Health University (Accession number 90, approved on 24 March 2010). All cases provided their written informed consent to participate in this study.

Fluorescent in situ hybridization (FISH). FISH was performed using a standard method. Briefly, PHA-stimulated lymphocytes or EB-transformed lymphoblasts were arrested by treatment with colcemid. Metaphase preparations were obtained by hypotonic treatment using 0.075 M KCl followed by methanol/acetate fixation. A 10 kb PstI fragment of HHV-6 was used as the probe (Fig. 1a)[3,12]. Probes were labeled by nick-translation with biotin-16-dUTP or digoxigenin-11-dUTP. After hybridization, the probes were detected using either Alexa Fluor® 488-conjugated streptavidin or rhodamine-conjugated anti-digoxigenin, respectively. Chromosomes were visualized by counter-staining with 4′,6-diamino-2-phenylindole (DAPI). As reference standards, we used RP11-186O8 (22q11.21), TelVysion 6p SpectrumGreen and TelVysion Xq/Yq SpectrumOrange (Abbott Molecular, IllinoisI, USA).

Multiplex ligation-dependent probe amplification (MLPA). MLPA probe pairs were designed using a standard methodology[22] so that they are strategically distributed throughout the viral genome, the central unique long (UL) region and two DRs, as well as pac1 and pac2. In this strategy, MLPA probes consist of two oligonucleotides, each containing a PCR primer sequence and a variable length sequence complementary to the target. Genomic DNA was denatured (1 min at 98°C) and subsequently hybridized to the MLPA probe pairs in accordance with the manufacturer's protocol (MRC-Holland, Amsterdam, Netherlands). After ligation, probe pairs were amplified using universal primers. The multiplex PCR products were then separated on a capillary sequencer. For normalization, we created a plasmid harboring a tandem array of probe sequences separated by 10-nucleotide spacer and used this construct as a standard for the copy number. We only had an EB-transformed cell line for case 63 and did not use this sample for MLPA because the presence of the EB virus genome may affect the results.

Analysis of junction fragments. Southern hybridization was performed using a standard methodology. Briefly, genomic DNA was cleaved with appropriate restriction enzymes, followed by size-separation via 0.8% agarose gel electrophoresis. After denaturation, the DNA was blotted onto a nylon membrane. Probes were labeled by crosslinking with alkaline-phosphatase and detected using CDP-Star detection reagent (GE Healthcare, Buckinghamshire, UK). To isolate a junction fragment, standard or long-range PCR was performed using LA Taq (TaKaRa, Siga, Japan). The amplification conditions were 35 cycles of 10 sec at 98°C, 30 sec at 63°C and 10 min at 72°C. A PCR primer was designed using the sequence data for the human chromosome X genomic contig (accession number NT_167191.1) and that of the HST strain of HHV-6B (AB021506). X-2R primer: 5′-TTGTCTCAGGGTCCTAGTG-3′. The PCR products were sequenced using the Sanger method.

Mapping of the distal breakpoints. To map distal breakpoints on the viral genomes, long-range PCR was performed using LA Taq. PCR primers were designed using the sequence data for the HST strain of HHV-6B (AB021506). The amplification conditions were 35 cycles of 10 sec at 98°C, 30 sec at 63°C and 10 min at 72°C. For amplification of larger fragments, PCR cycles were increased up to 38 cycles. To amplify telomere repeats, we performed the PCR using the Tel-A primer, 5′-CCCTAACCCTAACCCTAACCCTAACC-3′. To show the smear products really contain telomeric repeats Southern hybridization was performed with a telomere-specific probe[34].

1. Abtashi, D. V. *et al.* Human herpesvirus-6 strain groups: a nomenclature. *Arch Virol* **129**, 363–366 (1993).
2. Dominguez, G. *et al.* Human herpesvirus 6B genome sequence: coding content and comparison with human herpesvirus 6A. *J Virol* **73**, 8040–8052 (1999).
3. Isegawa, Y. *et al.* Comparison of the complete DNA sequences of human herpesvirus 6 variants A and B. *J Virol* **73**, 8053–8063 (1999).
4. Yamanishi, K. *et al.* Identification of human herpesvirus-6 as a causal agent for exanthem subitum. *Lancet* **1**, 1065–1067 (1988).
5. Yoshikawa, T. *et al.* Distribution of antibodies to a causative agent of exanthem subitum (human herpesvirus-6) in healthy individuals. *Pediatrics* **84**, 675–677 (1989).
6. Fox, J. D., Briggs, M., Ward, P. A. & Tedder, R. S. Human herpesvirus 6 in salivary glands. *Lancet* **336**, 590–593 (1990).

7. Kondo, K., Kondo, T., Okuno, T., Takahashi, M. & Yamanishi, K. Latent human herpesvirus 6 infection of human monocytes/macrophages. *J Gen Virol* **72 (Pt 6)**, 1401–1408 (1991).
8. Yoshikawa, T. *et al.* Human herpesvirus-6 infection in bone marrow transplantation. *Blood* **78**, 1381–1384 (1991).
9. Yoshikawa, T. Human herpesvirus 6 infection in hematopoietic stem cell transplant patients. *Br J Haematol* **124**, 421–432 (2004).
10. Morissette, G. & Flamand, L. Herpesviruses and chromosomal integration. *J Virol* **84**, 12100–12109 (2010).
11. Hall, C. B. *et al.* Chromosomal integration of human herpesvirus 6 is the major mode of congenital human herpesvirus 6 infection. *Pediatrics* **122**, 513–520 (2008).
12. Tanaka-Taya, K. *et al.* Human herpesvirus 6 (HHV-6) is transmitted from parent to child in an integrated form and characterization of cases with chromosomally integrated HHV-6 DNA. *J Med Virol* **73**, 465–473 (2004).
13. Pellett, P. E. *et al.* Chromosomally integrated human herpesvirus 6: questions and answers. *Rev Med Virol* **22**, 144–155 (2011).
14. Nacheva, E. P. *et al.* Human herpesvirus 6 integrates within telomeric regions as evidenced by five different chromosomal sites. *J Med Virol* **80**, 1952–1958 (2008).
15. Thomson, B. J., Dewhurst, S. & Gray, D. Structure and heterogeneity of the a sequences of human herpesvirus 6 strain variants U1102 and Z29 and identification of human telomeric repeat sequences at the genomic termini. *J Virol* **68**, 3007–3014 (1994).
16. Gompels, U. A. & Macaulay, H. A. Characterization of human telomeric repeat sequences from human herpesvirus 6 and relationship to replication. *J Gen Virol* **76 (Pt 2)**, 451–458 (1995).
17. de Lange, T. How telomeres solve the end-protection problem. *Science* **326**, 948–952 (2009).
18. Arbuckle, J. H. *et al.* The latent human herpesvirus-6A genome specifically integrates in telomeres of human chromosomes in vivo and in vitro. *Proc Natl Acad Sci U S A* **107**, 5563–5568 (2010).
19. Arbuckle, J. H. & Medveczky, P. G. The molecular biology of human herpesvirus-6 latency and telomere integration. *Microbes Infect* **13**, 731–741 (2011).
20. Tanaka, N. *et al.* Monitoring four herpesviruses in unrelated cord blood transplantation. *Bone Marrow Transplant* **26**, 1193–1197 (2000).
21. Achour, A. *et al.* Length variability of telomeric repeat sequences of human herpesvirus 6 DNA. *J Virol Methods* **159**, 127–130 (2009).
22. Schouten, J. P. *et al.* Relative quantification of 40 nucleic acid sequences by multiplex ligation-dependent probe amplification. *Nucleic Acids Res* **30**, e57 (2002).
23. Celli, G. B., Denchi, E. L. & de Lange, T. Ku70 stimulates fusion of dysfunctional telomeres yet protects chromosome ends from homologous recombination. *Nat Cell Biol* **8**, 885–890 (2006).
24. Celli, G. B. & de Lange, T. DNA processing is not required for ATM-mediated telomere damage response after TRF2 deletion. *Nat Cell Biol* **7**, 712–718 (2005).
25. Arbuckle, J. H. *et al.* Mapping the telomere integrated genome of human herpesvirus 6A and 6B. *Virology* **442**, 3–11 (2013).
26. Flamand, L., Komaroff, A. L., Arbuckle, J. H., Medveczky, P. G. & Ablashi, D. V. Review, part 1: Human herpesvirus-6-basic biology, diagnostic testing, and antiviral efficacy. *J Med Virol* **82**, 1560–1568 (2010).
27. Leong, H. N. *et al.* The prevalence of chromosomally integrated human herpesvirus 6 genomes in the blood of UK blood donors. *J Med Virol* **79**, 45–51 (2007).
28. Wang, X. & Baumann, P. Chromosome fusions following telomere loss are mediated by single-strand annealing. *Mol Cell* **31**, 463–473 (2008).
29. Hall, C. B. *et al.* Congenital infections with human herpesvirus 6 (HHV6) and human herpesvirus 7 (HHV7). *J Pediatr* **145**, 472–477 (2004).
30. Feschotte, C. & Gilbert, C. Endogenous viruses: insights into viral evolution and impact on host biology. *Nat Rev Genet* **13**, 283–296 (2012).
31. Linardopoulou, E. V. *et al.* Human subtelomeres are hot spots of interchromosomal recombination and segmental duplication. *Nature* **437**, 94–100 (2005).
32. De Bolle, L., Naesens, L. & De Clercq, E. Update on human herpesvirus 6 biology, clinical features, and therapy. *Clin Microbiol Rev* **18**, 217–245 (2005).
33. Kurahashi, H. *et al.* Recent advance in our understanding of the molecular nature of chromosomal abnormalities. *J Hum Genet* **54**, 253–260 (2009).
34. Ijdo, J. W., Wells, R. A., Baldini, A. & Reeders, S. T. Improved telomere detection using a telomere repeat probe (TTAGGG)n generated by PCR. *Nucleic Acids Res* **19**, 4780 (1991).

Acknowledgments

The authors thank Dr. Hiroshi Kogo and Makiko Tsutsumi for helpful discussions, Akiko Yoshikawa, Noriko Hayashizono and Narumi Kamiya for technical assistance. This work was supported by a grant-in-aid for Scientific Research from the Ministry of Education, Culture, Sports, Science, and Technology of Japan (24390085, 23659182, 23013019, http://www.mext.go.jp), and from the Ministry of Health, Labour and Welfare of Japan, to H.K (10103465, http://www.mhlw.go.jp).

Author contributions

T.O., T.Y. and H.K. conceived and designed the experiments. T.O. performed all the experiments. I.H., M.I., Y.H., K.K., J.O., H.Y., T.N., Y.T., S.K. and T.Y., contributed regents and materials. T.O. and H.K. wrote the manuscript. All authors reviewed the manuscript.

Additional information

Supplementary information accompanies this paper at http://www.nature.com/scientificreports

Competing financial interests: The authors declare no competing financial interests.

How to cite this article: Ohye, T. *et al.* Dual roles for the telomeric repeats in chromosomally integrated human herpesvirus-6. *Sci. Rep.* **4**, 4559; DOI:10.1038/srep04559 (2014).